A comparison between available potential and kinetic energy estimates for the southern and northern hemisperes

By P. G. PRICE, *Bureau of Meteorology, Melbourne, Australia*

(Manuscript received November 21, 1974)

ABSTRACT

A study is made of the zonal and eddy components of the quasi-geostrophic available potential and kinetic energies based on southern hemisphere data for the twelve-month period May 1972 to April 1973 and at the four levels 1 000, 500, 300 and 200 mb. Each component is found to show a late winter maximum and a summer minimum; however, their annual cycles appear less pronounced than those given by Wiin-Nielsen (1967) for the northern hemisphere. The eddy energies are subdivided into components associated with eddies of longitudinal wave numbers one to fifteen. The eddy spectra appear to follow simple power laws over the range of the smaller waves ($n \geq 7$): kinetic energy appears to follow a -3 relationship but the exponents for the available potential energy spectra are found to be closer to -4.

1. Introduction

The energetics of the northern hemisphere's circulation have been investigated extensively by many workers during recent years, especially following Lorenz's (1955) revival and extension to the whole atmosphere of Margules (1903) concept of the "available" energy of a storm as a small but vital fraction of its total energy. Research along these lines has been severely hampered in the southern hemisphere due to a lack of adequate data: most studies have been restricted to considerations of kinetic energies and have used the International Geophysical Year (IGY) (July 1957–December 1958) chart series which encompasses only the lower troposphere.

In a previous paper (Price, 1973), estimates of kinetic and available potential energy statistics based on the southern hemisphere analyses for the 18 months of the IGY were presented. As these analyses incorporate only the lower troposphere (the two fields analysed were mean sea level pressure and 500 mb geopotential height) the results were recognised as being of only limited value and it was stated then that similar computations based on data sets more extensive in time and (vertical) space, should be made in order to build up a more realistic climatology of the energetics of the southern hemisphere's circulation.

The implementation during 1972 of a full numerical analysis programme at the Melbourne World Meteorological Centre (WMC) has now produced a multilevel data set which affords the opportunity of extending our knowledge of this hemisphere's dynamic climatology beyond that previously available. A general description and operational evaluation of the analysis–prognosis system used at the Melbourne WMC to produce the archived analyses used in this study are given by Gauntlett et al. (1972).

2. Equations, data and procedure

The contributions to the total, zonal and eddy components of the kinetic and available potential energies (K, K_Z, K_E and A, A_Z, A_E respectively) by the layer of pressure thickness Δp were computed using equations similar to those used, for example, by Wiin-Nielsen (1964) viz.

$$K = K_Z + K_E = K_Z + \sum_1^\infty K_n$$

$$A = A_Z + A_E = A_Z + \sum_1^\infty A_n$$

where

$$K_Z = \frac{\Delta p g \pi}{2f^2 S} \int_{\phi_1}^{\phi_2} [(\partial \alpha_0/\partial \phi)^2 + (\partial a_0/\partial \phi)^2] \cos \phi \, d\phi$$

$$A_Z = \frac{a^2 g \pi}{\bar{\sigma} \Delta p S} \int_{\phi_1}^{\phi_2} [(a_0 - z) - (\alpha_0 - Z)]^2 \cos \phi \, d\phi$$

$$K_n = \frac{\Delta p g \pi}{4f^2 S} \int_{\phi_1}^{\phi_2} [(\partial \alpha_n/\partial \phi)^2 + (\partial a_n/\partial \phi)^2 + (\partial \beta_n/\partial \phi)^2 + (\partial b_n/\partial \phi)^2 + n^2(\alpha_n^2 + a_n^2 + \beta_n^2 + b_n^2)/\cos^2\phi] \cos \phi \, d\phi$$

$$A_n = \frac{a^2 g \pi}{2\bar{\sigma} \Delta p S} \int_{\phi_1}^{\phi_2} [(a_n - \alpha_n)^2 + (b_n - \beta_n)^2] \cos \phi \, d\phi$$

In these equations, a_0, a_n, b_n and α_0, α_n, β_n are the latitudinal Fourier coefficients of the heights of the lower and upper boundaries of the layer and z, Z their area means; $\bar{\sigma}$ is an average value of static stability, a function of pressure only; S is the area and ϕ_1, ϕ_2 are the latitudinal boundaries of the region under consideration; a is the earth's radius; n is longitudinal wave number, and f is a mean value of the coriolis parameter.

The basic data consisted of grid point values of daily mean sea level pressures and geopotential heights at 500, 300 and 200 mb on the standard 47 × 47 analysis grid for the period May 1, 1972 to April 30, 1973. Data were missing on 17 days during this period due to a variety of operational reasons. To facilitate the adaptation of existing computer programmes, for those dates the data were assumed to be identical to those of the previous day. As at most three days data were missing during any month, this simplification should not significantly affect the results presented here.

The data were interpolated from the analysis grid to a latitude/longitude grid with a latitudinal increment of 5 deg and a longitudinal increment of 10 deg extending from 10° S to 70° S. Although almost 80 % of the hemisphere is contained in this belt, the undoubtedly important contributions by the polar and equatorial regions have been neglected in these results. This was thought necessary because of the decreasing reliability of analysis over the equatorial belt at all levels and over the high latitudes, particularly in the lower troposphere where the pressure surfaces are generally ficticious. Special attention should be given to these aspects at a further stage in this project.

The same procedure for the calculation of the energy terms was adopted for each pair of pressure levels (1 000–500 mb, 500–300 mb and 300–200 mb) as was applied to the IGY mean sea level and 500 mb data using appropriate values of static stability and layer pressure thickness in the above equations.

The daily values and monthly, seasonal ("winter": May 1, 1972 to September 30, 1972, "summer": November 1, 1972 to March 31, 1973) and annual (May 1, 1972 to April 30, 1973) means of the above energies were computed for each layer and, by extrapolation, for the total layer 1 000–0 mb. The eddy energies associated with the waves of various number —K_n, A_n—were calculated for $n = 1$ to 15, the latter corresponding roughly to the smallest scale resolvable in a hemispheric analysis. Monthly, seasonal and annual means of K_Z, K_E, K_n and A_Z, A_E, A_n for the layer 1 000–0 mb are given in Table 1.

3. Discussion

Comparisons will be made between southern hemisphere estimates and corresponding similar results for the northern hemisphere:

(*a*) by Wiin-Nielsen (1967) based on NMC Washington analyses at 8 pressure levels—1 000, 850, 700, 500, 300, 200, 150 and 100 mb—covering the period February 1963 to January 1964 and extending from 17.5° N to 87.5° N; and

(*b*) by Saltzman (1970) and Oort (1964) which are those authors' estimates of most probable values selected during critical surveys of the results published by several investigators.

All results are expressed as either kJm^{-2} (energy/unit area) or $kJm^{-2} cb^{-1}$ (energy/unit area/unit pressure layer) and, when appropriate, diagrams plotted so that the seasons in each hemisphere are aligned. As a consequence, Wiin-Nielsen's results are plotted in the sequence November 1963 to January 1964, February 1963 to October 1963.

Several estimates of the annual means of the total zonal and eddy energies for the layer 1 000 to 0 mb are given in Table 2 whilst the variations throughout the year of each of the

Table 1. *Monthly, seasonal and annual means of A_Z, A_E, A_n and K_Z, K_E and K_n for the southern hemisphere. Units: kJm^{-2}*

	May	June	July	Aug.	Sept.	Oct.	Nov.	Dec.	Jan.	Feb.	Mar.	April	Summer	Winter	Year
K_Z	953	869	1 103	1 015	1 215	1 158	1 060	808	906	1 019	1 043	1 030	964	1 031	1 013
K_1	105	107	101	130	69	94	79	63	40	46	69	74	60	103	82
K_2	76	90	91	74	58	61	33	64	45	50	44	76	47	78	63
K_3	122	131	85	87	78	68	63	58	52	104	70	91	69	101	84
K_4	98	129	95	155	85	105	85	76	68	85	64	103	76	112	96
K_5	90	80	106	129	93	75	88	55	63	57	69	73	66	100	81
K_6	86	93	74	80	110	76	55	81	60	82	65	69	70	89	78
K_7	51	60	113	69	75	64	46	54	59	37	38	58	48	74	60
K_8	35	47	53	43	40	62	28	46	36	31	31	36	33	45	39
K_9	31	38	38	34	33	34	27	27	22	20	25	28	24	35	30
K_{10}	22	20	27	21	21	20	17	18	16	17	16	23	17	23	20
K_{11}	16	20	18	22	13	15	13	12	10	12	15	15	12	18	15
K_{12}	13	16	15	15	11	9	10	9	9	8	9	14	9	14	12
K_{13}	9	11	10	13	10	8	7	6	6	7	8	10	7	10	9
K_{14}	7	10	9	9	7	6	7	6	6	5	6	9	6	8	7
K_{15}	7	8	8	8	6	6	5	5	5	6	5	6	5	7	6
$K_E = \Sigma_1^{15} K_n$	768	860	843	889	709	703	563	580	497	566	534	685	549	817	682
A_Z	4 640	4 343	5 413	5 391	5 521	5 060	4 431	3 935	4 152	4 126	4 318	4 377	4 193	5 022	4 652
A_1	117	139	132	146	100	106	64	61	55	62	72	90	63	126	95
A_2	74	73	76	61	60	54	38	47	51	51	36	57	45	69	57
A_3	85	81	65	87	62	57	49	37	39	76	57	63	41	76	63
A_4	63	55	55	77	52	88	54	59	56	62	61	60	58	60	61
A_5	58	35	46	53	62	47	49	31	40	42	38	44	40	51	45
A_6	40	34	36	36	57	44	31	35	31	40	36	31	35	40	38
A_7	23	23	44	27	32	29	20	18	23	17	16	23	19	30	25
A_8	16	15	24	16	15	19	13	14	12	13	11	13	12	17	15
A_9	14	15	11	9	10	12	8	8	6	8	9	9	8	11	10
A_{10}	9	6	7	8	6	7	5	5	5	5	5	7	5	7	6
A_{11}	6	5	5	5	4	4	4	3	3	3	3	5	3	5	4
A_{12}	4	3	4	4	3	3	3	2	2	3	2	3	2	4	3
A_{13}	3	3	3	3	3	2	2	2	1	2	2	3	2	3	2
A_{14}	2	2	3	2	2	2	2	1	1	1	2	2	1	2	2
A_{15}	2	2	2	2	2	1	1	1	1	1	1	1	1	2	1
$A_E = \Sigma_1^{15} A_n$	516	491	513	536	470	475	343	324	326	386	351	411	345	503	427

southern hemisphere estimates are compared with those of Wiin-Nielsen (1967) in Fig. 1.

These results suggest three major inter-hemispheric differences, all of which are probably consequences of their basic oceanic and continental dissimilarities:

(*a*) although both hemispheres' energies show maxima during late winter and minima during summer, their annual cycles are much more pronounced in the northern hemisphere;

(*b*) the total energy ($A + K$) is greater in the southern than the northern hemisphere, mainly because, in the former, A (through its zonal component) is much greater;

(*c*) a greater proportion of each energy is contained in the zonal components in the southern hemisphere.

A_Z is essentially a measure of the strength of north-south thermal gradients and in Fig. 2, the long term mean zonally averaged latitudinal profiles from latitudes 10° to 70° of 700, 500 and 400 mb temperatures (taken from Palmén & Newton (1969))—the levels contributing most to A_Z—are presented. It can be seen that the gradients are essentially similar for each hemisphere during winter; they are weaker during summer in both but the southern gradients are considerably stronger than those of the northern hemisphere. Thus, a lower amplitude cycle would be expected in A_Z (and K_Z) in the south-

Table 2. *Annual means of* A, A_Z, A_E *and* K, K_Z, K_E *for the northern hemisphere (Oort (1964), Saltzman (1970) and Wiin-Nielsen (1967)) and southern hemisphere (this study). Units* kJm^{-2}

The figures in brackets express each energy as a percentage of the corresponding value from this study

	A_Z	A_E	$A = A_Z + A_E$	K_Z	K_E	$K = K_Z + K_E$	$T = K + A$
Oort	4 000	1 500	5 500	800	700	1 500	7 000
	±1 000	±500	±1 500	±300	±300	±600	±2 100
	(86)	(351)	(108)	(79)	(103)	(88)	(103)
Saltzman	2 900	900	3 800	800	1 200	2 000	5 800
	(62)	(211)	(75)	(79)	(176)	(118)	(86)
Wiin-Nielsen	3 165	814	3 979	832	1 017	1 849	5 828
	(68)	(191)	(78)	(82)	(149)	(109)	(86)
This study	4 652	427	5 079	1 013	682	1 695	6 774
	(100)	(100)	(100)	(100)	(100)	(100)	(100)

ern hemisphere and hence its annual mean zonal energies should be greater.

The stronger zonality of the southern hemisphere's circulation also suggests that its zonal components would be stronger than the northern hemisphere values. This is particularly evident in A: only about 75 to 80% of the northern hemisphere's annual mean available potential energy is contained in A_Z whilst in the southern hemisphere, more than 90% of it is zonal.

The ratios of the monthly means of total kinetic energy to total available potential energy are shown in Fig. 3 for each hemisphere: it can be seen that a greater fraction of the total energy is kinetic in the northern than the southern hemisphere throughout the year. As well, the former's ratio displays a marked annual cycle in phase with the energy cycles themselves in that K is more than half the magnitude of A in winter but less than 40% of it during summer. In the southern hemisphere, the ratio remains fairly constant throughout the year ranging from 0.36 in April to 0.29 in January. All values are considerably greater than Lorenz's (1955) original order of magnitude estimate of about 0.1.

The various components are shown as functions of pressure and time in Fig. 4*a*–*d*. In preparing these diagrams, the southern hemisphere values have been attributed to the mid-points of appropriate layers and the isopleths have been restricted to pressures between about 250 mb and 800 mb. They are compared with similar figures for the northern hemisphere presented by Wiin-Nielsen (1967). Note that more detail will be contained in the latter as a result of the finer vertical resolution in Wiin-Nielsen's data. The following broad features can be noted:

(*a*) A_Z (Fig. 4*a*): The primary southern hemisphere maximum occurs in the middle troposphere during late winter, somewhat later than in the northern hemisphere whilst both hemispheres show minima during summer in the lower layers and markedly decreasing values above 400 mb. Values are of the same order in both hemispheres, at all levels.

(*b*) A_E (Fig. 4*b*): Winter maxima around the mid troposphere, and low level summer minima appear in both hemispheres. The southern hemisphere values show a more pronounced decrease above 400 mb; as well, they are about 30 to 50% of corresponding northern hemisphere values.

(*c*) K_Z (Fig. 4*c*): As with A_Z, the main southern hemisphere maximum is seen during late winter, again somewhat later than for the northern hemisphere. The highest southern hemisphere values observed are near 200 mb but the data are insufficient to show if K_Z decreases at higher levels as is observed in the northern hemisphere, although this is doubtless the case. In both hemispheres a minimum of K_Z occurs at all levels during summer, whilst values at low levels are seen to be a small fraction of the 200 mb value for the same time. The regions in each hemisphere for which K_E exceeds K_Z are also indicated in Fig. 4*c*. It can be seen that this condition occurs more fre-

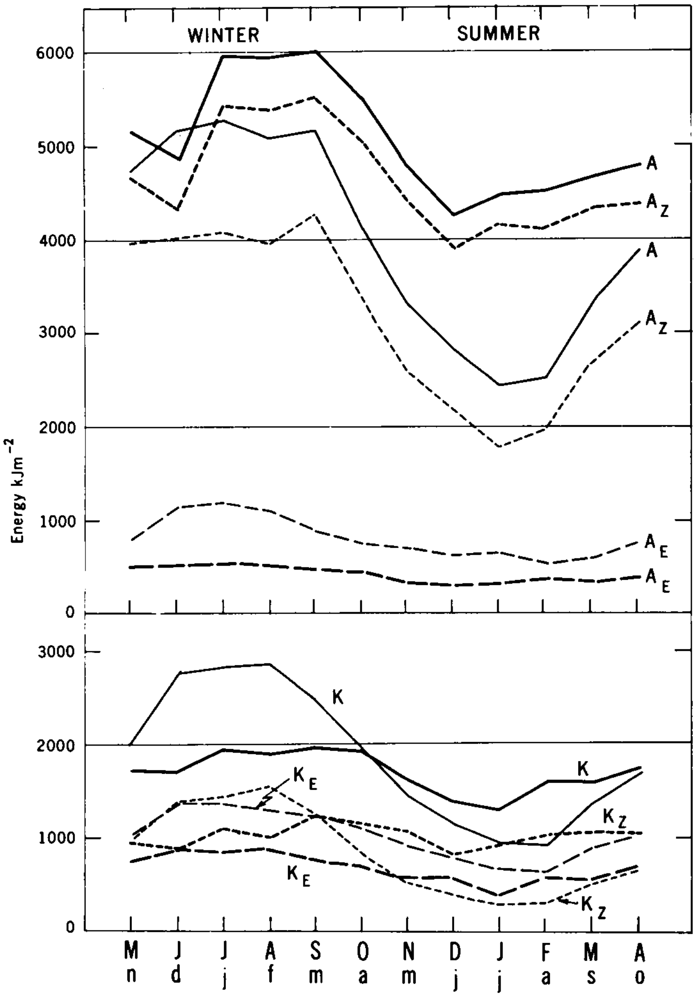

Fig. 1. Monthly mean values of A, A_Z, A_E and K, K_Z, K_E for the layer 1 000–0 mb for the northern hemisphere after Wiin-Nielsen (1967) (thin lines) and the southern hemisphere from this study (bold lines). The northern hemisphere values have been rearranged so that seasons correspond. Months are indicated in upper and low cases for the southern and northern hemispheres respectively. Units: kJm^{-2}.

quently and to a greater vertical extent in the northern than southern hemisphere.

(*d*) K_E (Fig. 4*d*). As with K_Z, maxima appear in both hemispheres during winter; however, although that of the northern hemisphere occurs lower than the corresponding K_Z maximum (near 300 mb, compared to near 200 mb) the southern hemisphere maximum is at 200 mb and is not shown to be an absolute one. In other aspects, the isopleths of K_E resemble those of K_Z.

The mean southern hemisphere annual, summer and winter spectra of K_E and A_E as functions of wave number are shown in Fig. 5. They are compared with similar spectra for the northern hemisphere as given by Wiin-Nielsen (1967) and Saltzman (1970).

As would be expected from the discussion on total eddy energies given above, the northern hemisphere eddy energies are, in general, greater than those for the southern hemisphere at corresponding wave numbers. As well, the following features are noteworthy:

(*a*) The K_E spectra in the southern hemisphere show absolute maxima at wave number 4 and secondary maxima, almost the same size at

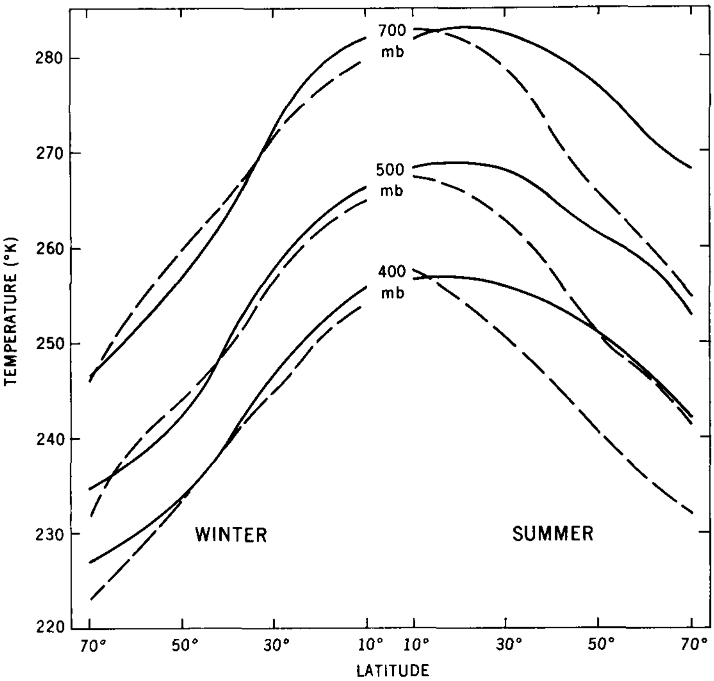

Fig. 2. Long term mean zonally averaged meridional profiles of 700, 500 and 400 mb temperatures between latitudes 10° and 70° (after Palmén & Newton (1969)); southern hemisphere, broken lines; northern hemisphere, solid lines. Units: deg K.

wave number 1. In the northern hemisphere, the primary maxima occur at lower wave numbers with secondary maxima apparent to wave numbers as high as eight.

(*b*) The A_E spectra show absolute maxima in both seasons and hemispheres at wave number 1; the southern hemisphere shows another maximum at wave number 3 in winter (considerably

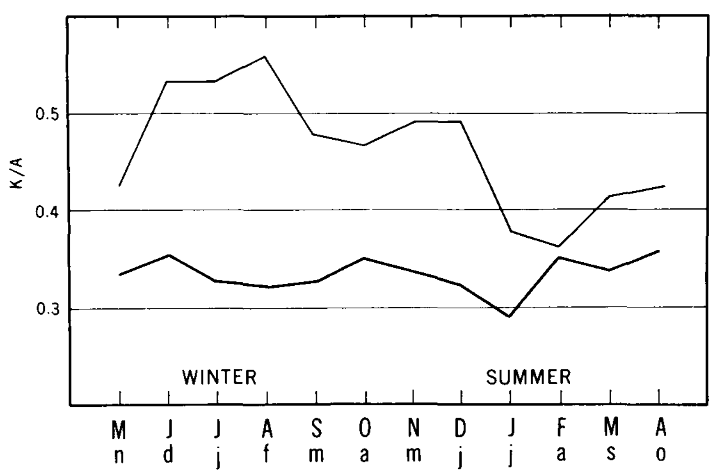

Fig. 3. Ratios of the monthly means of total kinetic energy (K) to total available potential energy (A) for the northern hemisphere after Wiin-Nielsen (1967) (thin line) and the southern hemisphere from this study (bold line). The northern hemisphere values have been rearranged so that seasons correspond. Months are indicated in upper and low cases for the southern and northern hemispheres respectively.

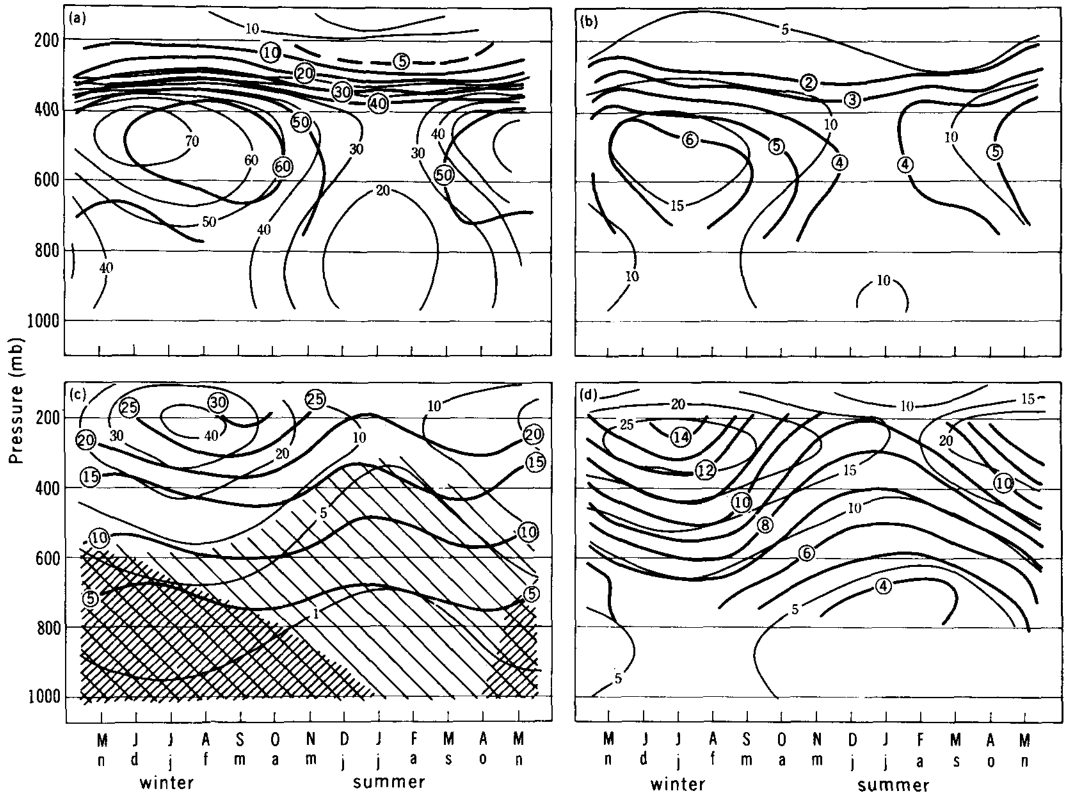

Fig. 4. Energies shown as functions of pressure and times: (*a*) A_Z; (*b*) A_E; (*c*) K_Z; (*d*) K_E. Southern hemisphere data from this study are analysed as bold isopleths with circled labels; northern hemisphere data after Wiin-Nielsen (1967), as thin isopleths with uncircled labels. The pressures and months for which K_E exceeds K_Z are shown in (*c*) as single and cross hatching respectively for the southern and northern hemispheres. The northern hemisphere values have been rearranged so that seasons correspond. Months are indicated in upper and low cases for the southern and northern hemispheres respectively. Units: $\mathrm{kJm^{-2}cb^{-1}}$.

less than the absolute maximum) and at wave number 4 in summer (almost the same as the absolute maximum).

(*c*) Spectra for both energy forms appear to be divided into two sections at around wave number 6 to 8: the longer waves (wave numbers 1 to 6) contain the bulk of K_E and A_E and are characterised by sharp variations in energy; the shorter waves (wave numbers 8 to 15) are characterised by steady decreases in energy with increasing wave number.

The partitioning into the two characteristic sections is revealed more dramatically by plotting the spectra on logarithmic axes: this is shown in Fig. 6. A least squares linear regression line has been fitted in the range of wave numbers 7 to 15. These lines are of the form

$$E = bn^{-\alpha}$$

where E is K_n or A_n and α and b are constants. Values of α for various layers and periods are compared in Table 3 with some northern hemisphere estimates.

It can be seen that in the case of K_n, the exponents in the southern hemisphere are close to -3, the value suggested by theoretical considerations (see e.g. Leith, 1968), and not considerably greater than the values found in the northern hemisphere. However, A_n shows a considerably more rapid decay in the southern hemisphere than in the northern hemisphere in the lower troposphere where values of α were respectively near 4 and from 2.5 to 3.5. This may be related to the fact that A_E is much smaller in the southern than northern hemisphere. No estimate can be made at this stage of the upper limit of wave number (beyond 15) for which these laws may apply.

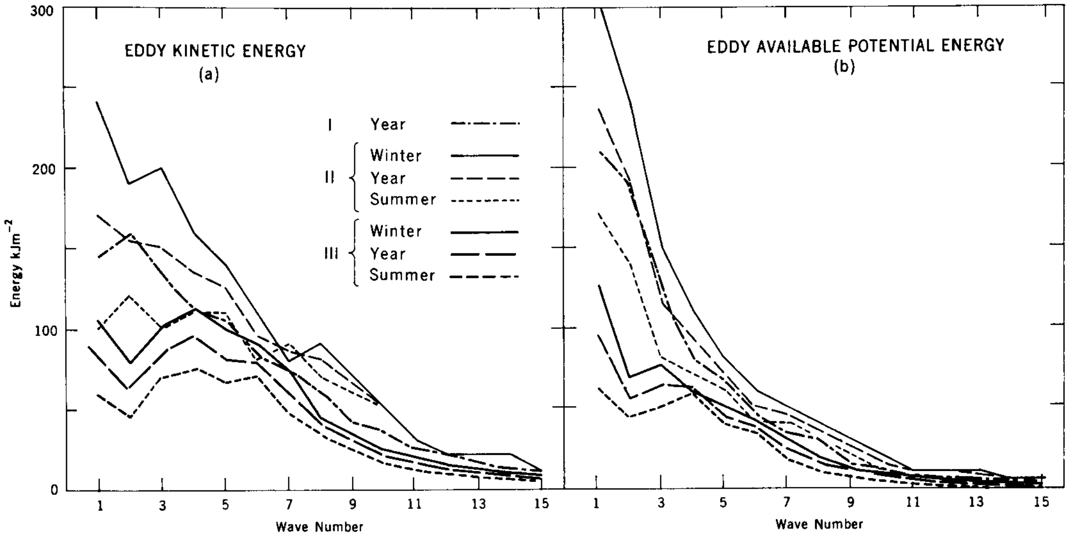

Fig. 5. Mean annual, winter and summer spectra of (*a*) eddy kinetic energy and (*b*) eddy available potential energy for (i) the northern hemisphere. (I) after Wiin-Nielsen (1967); (II) after Saltzman (1970) and (ii) the southern hemisphere. (III) this study. Units: kJm^{-2}.

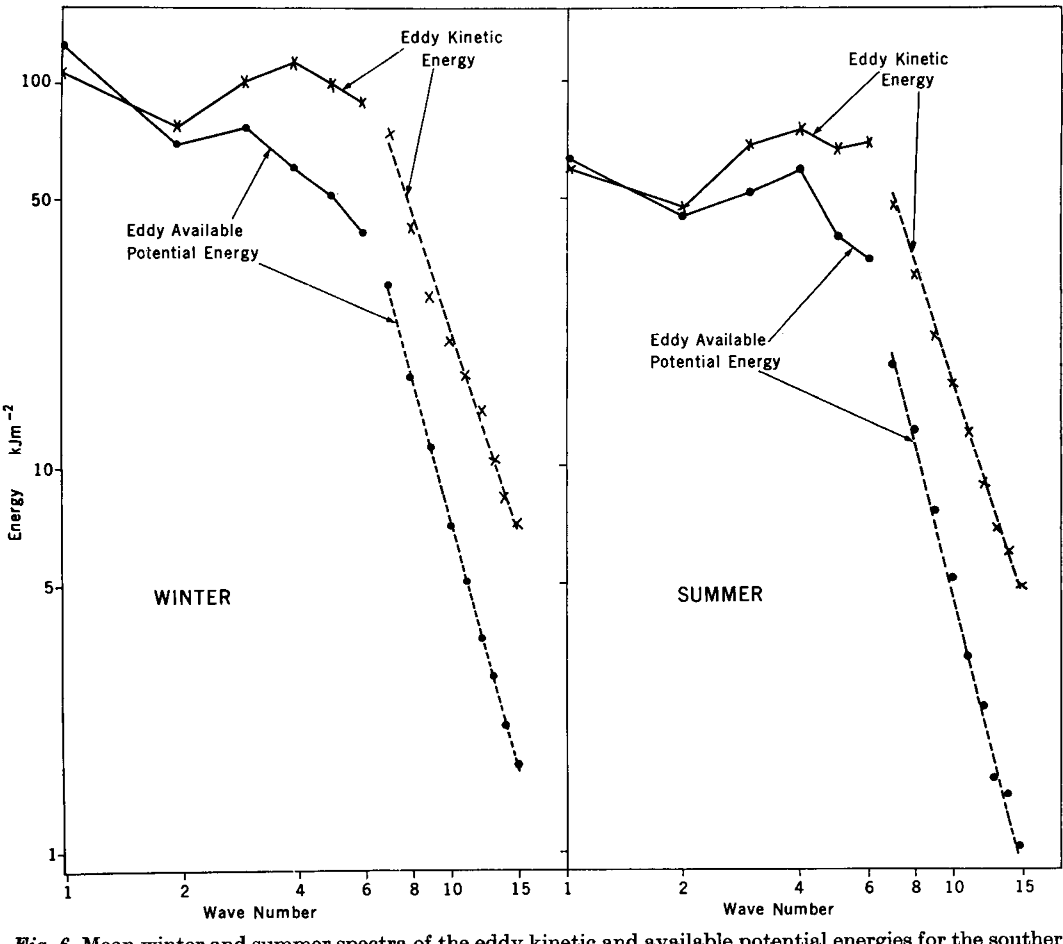

Fig. 6. Mean winter and summer spectra of the eddy kinetic and available potential energies for the southern hemisphere plotted on logarithmic axes. Values are joined for wave numbers 1 to 6; the linear regression line is shown for wave numbers 7 to 15. Units: kJm^{-2}.

4. Concluding remarks

Some preliminary steps have been taken in this study towards building up a dynamic climatology of the general circulation of the southern hemisphere and the statistics presented should serve as a useful guide to the performance of numerical models which are being applied to studying it. As they are based on a relatively short period, it is important that studies similar to this are repeated as more data are produced at the Melbourne WMC, until a reliable long term climatology has been deduced. However, account will need to be taken of the impacts of changing analysis and observing systems during the period of data accumulation. For example, any significantly improved specification of the smaller scales of the circulation by the use of satellite soundings may result in spectral distributions of eddy energies markedly different from those presented in Figs. 5 and 6.

The statistics have been compared with similar estimates for the northern hemisphere presented by Oort (1964), Wiin-Nielsen (1967), and Saltzman (1970) and, to the extent that any can be considered representative of the appropriate hemispheric climatology, the following conclusion can be made:

(*a*) the total energy $(A+K)$ is greater in the southern than the northern hemisphere;

(*b*) the southern hemisphere energies exhibit less pronounced annual cycles than those of the northern hemisphere;

(*c*) the zonal components of each energy are greater in the southern than in the northern hemisphere; and

(*d*) kinetic energy makes a smaller contribution to the total energy in the southern than in the northern hemisphere.

A breakdown of the southern hemisphere eddy energies into their components associated with waves of different size reveals the apparent importance in the southern hemisphere of wave number 4 and that a simple power law relates the energies associated with the smaller waves $(n \geqslant 7)$ and their wave numbers. The power law exponent is about -3 for eddy kinetic energy but is nearer -4 for eddy available potential energy.

Table 3. *Values of α in the equation $E = bn^{-\alpha}$ for (a) the northern hemisphere. (A) annual means after Wiin-Nielsen (1967); (B) winter means after Horn & Bryson (1963) (taken as arithmetic means of values found at 25°, 45° and 65° N) and (b) the southern hemisphere: (C) IGY annual means, after Price (1973); (D) annual means, this study*

	A	*B*		*C*	*D*
Eddy kinetic energy					
1 000–925	1.9		1 000–500	2.9	3.0
925–775	2.4				
775–600	2.6	2.4			
600–400	2.9	2.6	500–300		3.2
400–250	3.1	2.7	300–200		3.1
250–100	2.8				
Mean 1 000–200	2.8		Mean 1 000–200		3.1
Eddy available potential energy					
1 000–850	2.4		1 000–500	3.9	4.1
850–700	2.8				
700–500	3.3				
500–300	3.5		500–300		3.4
300–200	2.7		300–200		3.4
200–150	3.5				
150–100	3.3				
Mean 1 000–100	3.2		Mean 1 000–200		3.8

Acknowledgements

Mr A. G. Davies was responsible for overall coordination of the support by the ADP Branch of the Bureau of Meteorology for this study whilst Messrs R. Riedell, K. V. Seaman and R. G. Seecamp each made substantial contributions to the actual programming. The author acknowledges with gratitude their assistance. The paper is published by permission of the Director of Meteorology, Australia.

REFERENCES

Gauntlett, D. J., Seaman, R. S., Kininmonth, W. R. & Langford, J. C. 1972. An operational evaluation of a numerical analysis prognosis system for the southern hemisphere. *Australian Meteorological Magazine 20*, 61–82.

Horn, L. H. & Bryson, R. A. 1963. An analysis of

the geostrophic kinetic energy spectrum of large-scale atmospheric turbulence. *Journal of Geophysical Research 68*, 1059–1064.
Leith, C. E. 1968. Diffusion approximation for two dimensional turbulence. *Physics of Fluids 11*, 671–673.
Lorenz, E. N. 1955. Available potential energy and the maintenance of the general circulation. *Tellus 1*, 157–167.
Margules, M. 1903. On the energy of storms. Appearing as a translation by C. Abbe in: *Smithsonian miscellaneous collections, 51*, (1910) 533–595.
Oort, A. H. 1964. On estimates of the atmospheric energy cycle. *Monthly Weather Review 92*, 483–493.
Palmén, E. & Newton, C. E. 1969. *Atmospheric circulation systems*. Academic Press, New York. 603 pp.
Price, P. G. 1973. On the available potential and kinetic energies of the lower troposphere in the southern hemisphere. *Australian Meteorological Magazine 21*, 29–45.
Saltzman, B. 1970. Large scale atmospheric energetics in the wave number domain. *Review of Geophysics and Space Physics 8*, 289–302.
Wiin-Nielsen, A. 1964. Some new observational studies of energy and energy transformations in the atmosphere. *WMO Tech. Note 66*, 177–202.
Wiin-Nielsen, A. 1967. On the annual variation and spectral distribution of atmospheric energy. *Tellus 19*, 540–559.

СРАВНЕНИЕ МЕЖДУ ОЦЕНКАМИ ДОСТУПНОЙ ПОТЕНЦИАЛЬНОЙ И КИНЕТИЧЕСКОЙ ЭНЕРГИИ ДЛЯ ЮЖНОГО И СЕВЕРНОГО ПОЛУШАРИЙ

На основе данных на 4-х уровнях 1 000, 500, 300 и 200 *мб* для южного полушария за период 12 месяцев с мая 1972 г. по апрель 1973 г. изучаются зональная и вихревая компоненты квазигеострофической доступной потенциальной энергии и кинетической энергии. Найдено, что каждая компонента выявляет максимум в конце зимы и минимум летом; однако их годовой ход выражен не так сильно, как это было найдено Вийн-Нильсеном (1967) для северного полушария. Вихревые энергии подразделяются на компоненты, связанные с вихрями с долготными волновыми числами от 1 до 15. Спектры этих вихрей представляются следующими простым степенным законам в интервале меньших длин волн ($n \geq 7$): кинетическая энергия падает с ростом n с показателем, близким к -3, однако, показатели степени для спектров доступной потенциальной энергии ближе к -4.